

9. Ворошнин Л.Г. Перспективы развития химико-термической обработки // Упрочняющие технологии и покрытия. – 2008. – №1. – С. 5 – 8.
10. Гурьев А. М., Лыгденов Б. Д., Попова Н. А., Козлов Э. В. Физические основы химико-термоциклической обработки сталей. – Барнаул: Изд-во АлтГТУ, -2008. – 250 с.
11. Власова О.А., Иванов С.Г., Гурьев А.М., Кошелева Е.А., Чех С.А. Оптимизация многокомпонентной химико-термической обработки стали 30X // Современные наукоёмкие технологии. – №3, – 2008, – С 54 – 55.
12. Иванов С.Г., Гурьев А.М., Кошелева Е.А., Власова О.А., Гурьев М.А. Комплексное насыщение сталей бором и хромом – борохромирование // Ползуновский альманах. – 2008. – № 3. – С. 53.
13. Гурьев А.М., Грешилов А.Д., Кошелева Е.А., Иванов С.Г., Гурьев М.А., Иванов А.Г., Долгоров А.А. Многокомпонентное диффузионное упрочнение поверхности деталей машин и инструмента из смесей на основе карбида бора // Обработка металлов. – №2.- 2010.- С. 19-23.
14. Гурьев А.М., Иванов С.Г., Гурьев М.А., Иванов А.Г., Лыгденов Б.Д., Земляков С.А., Долгоров А.А. Структура и свойства упрочненных бором и бором совместно с титаном поверхности штамповых сталей 5ХНВ и 5Х2НМВФ // Фундаментальные проблемы современного материаловедения. – 2010. Т. 7. – № 1. -С. 27-31.
15. Гурьев М.А., Иванов С.Г., Кошелева Е.А., Иванов А.Г., Грешилов А.Д., Гурьев А.М., Лыгденов Б.Д., Околович Г.А. Комплексное диффузионное упрочнение тяжело нагруженных деталей машин и инструмента // Ползуновский вестник. - 2010. -№ 1. – С. 114-121.
16. Гурьев М.А., Гурьев А.М., Иванов А.Г., Иванов С.Г. Анализ влияния природы легирующих элементов в высоколегированных сталях на процессы комплексного многокомпонентного диффузионного борирования // Международный журнал прикладных и фундаментальных исследований. 2010. – № 5. – С. 155-157.
17. Гурьев А.М., Иванов С.Г., Грешилов А. Д., Земляков С.А. Механизм образования боридных игл при диффузионном комплексном борохромировании из насыщающих обмазок // Обработка металлов (технология, оборудование, инструменты). – 2011. – № 3. – С. 34-40.
18. Иванов С.Г., Гармаева И.А., Андросов А.П., Зобнев В.В., Гурьев А.М., Марков В.А. Фазовые превращения и структура комплексных боридных покрытий // Ползуновский вестник. – 2012. – № 1-1. – С. 106-108.
19. Гурьев М.А., Фильчаков Д.С., Гармаева И.А., Иванов С.Г., Гурьев А.М., Околович Г.А. Технология нанесения многокомпонентных упрочняющих покрытий на стальные детали // Ползуновский вестник. – 2012. – № 1-1. – С. 73-78.
20. Иванов С.Г., Гурьев А.М., Русакова А.В., Гурьев М.А., Старостенков М.Д. Микроструктура поверхности многокомпонентных диффузионных покрытий на основе бора // Фундаментальные проблемы современного материаловедения. – 2013. Т. 10. – № 1. – С. 130-133.
21. Иванов С.Г., Гармаева И.А., Гурьев М.А., Гурьев А.М. Особенности многокомпонентного насыщения легированных сталей // Современное машиностроение. Наука и образование. – 2013. – № 3. – С. 1155-1160.
22. Гурьев А.М., Лыгденов Б.Д., Гурьев М.А., Шунчи М., Власова О.А. Борирование малоуглеродистой стали. – Raleigh, North Carolina, USA: Lulu Press, -2015. – 141p.
23. Логинова М.В., Иванов С.Г., Яковлев В.И., Гурьев М.А., Дон Яджи, Гурьев А.М. Фазовый состав композиционных покрытий на углеродистых сталях // Фундаментальные проблемы современного материаловедения, – 2015. -№1,- С.99-102.

Сведения об авторах

А.М. Гурьев, д.т.н., профессор, Алтайский государственный технический университет им. И.И. Ползунова, Барнаул, Россия, 656038, Алтайский край, тел.+7 (3852) 29-07-06 пр. Ленина, д.46, профессор Уханьский текстильный университет, Ухань, Китай e-mail: gurievam@mail.ru

С.Г. Иванов, к.т.н., Алтайский государственный технический университет, Барнаул, Россия, 656038, Алтайский край, тел.+7 (3852) 29-07-06 пр. Ленина, д.46.

М.А. Гурьев, к.т.н., докторант, Алтайский государственный технический университет, Барнаул, Россия, 656038, Алтайский край, тел.+7 (3852) 29-07-06 пр. Ленина, д.46.

Б.Д. Лыгденов, д.т.н., профессор Восточно-Сибирский государственный университет технологий и управления, Улан-Удэ, 670013, ул.Ключевская 40в, Россия, профессор Уханьский текстильный университет, Ухань, Китай, e-mail: lygdenov59@mail.ru.

Мэй Шунчи, профессор Уханьский текстильный университет, Ухань, Китай, e-mail: 1533876320@qq.com.

УДК 539.23

doi:10.18.101/978-5-9793-0883-8-94-98

Towards Multidimensional Carbon Materials: Turning Graphene into Thin Diamond Nanostructures

Dorj Odkhuu¹, Noejung Park², Rodney. S. Ruoff³,

¹Department of Physics, Incheon National University, Academy-ru 119, Incheon 460-772, Republic of Korea,
e-mail: odkhuu@inu.ac.kr

²Department of Physics, Ulsan National Institute of Science and Technology (UNIST), Ulsan 689-798, Korea,
e-mail: noejung@unist.ac.kr

³Department of Mechanical Engineering and the Materials Science and Engineering Program, The University of Texas,
Austin, Texas 78712, United State of America, email: r.ruoff@mail.utexas.edu

Abstract

Herein, we demonstrate a preferable synthetic route to transform sp^2 graphene layers into nanoscale-thick diamond nanostructures. The ultrathin purely sp^3 bonded carbon diamond can be easily produced through the functionalization of the outer wall of graphene layers on a metal surface without the need of so called high pressure and high temperature (HPHT) circumstance. The resulting ultrathin sp^3 carbon films are not only diamond per se, but rather are a new material that is only of order ~ 1 nanometer in thickness. This approach is also applicable to a *hexagonal* layered boron nitride.

Keywords: Graphene, thin diamond nanostructure, sp^2 - sp^3 transformation.

Многомерные углеродные материалы с включением графена в разреженных бриллиантовых наноструктурах

Дорж Одкху¹, Ноеджун Парк², Родни. С. Руофф³,

¹Физический факультет, Инчхонский национальный университет, Академия-ру 119, Инчхон 460-772, Республика Корея, электронная почта: odkhuu@inu.ac.kr

²Физический факультет, Ульсанский национальный институт науки и технологий (UNIST), Ульсан 689-798, Корея, электронная почта: noejung@unist.ac.kr

³Факультет машиностроения и научно-технической программы материалов, Университет Техаса, Остин, штат Техас 78712, Соединенные Штаты Америки штат, электронная почта: r.ruoff@mail.utexas.edu

Аннотация

В данной статье рассматривается путь синтеза для преобразования sp^2 слоев графена в наноразмерных алмазных наноструктурах. Ультратонкий sp^3 алмазный углерод может быть легко получен путем функционализации наружной стенки графеновых слоев на металлической поверхности без необходимости так называемого высокого давления и высокой температуры (HPHT). Полученные ультратонкие sp^3 углеродные пленки представляют собой не только алмаз, а скорее представляют новый материал, порядка ~ 1 нанометра в толщину. Этот подход также применим к гексагональному слоистому нитриду бора.

Ключевые слова: графен, тонкие алмазные наноструктуры, sp^2 - sp^3 гибридизация.

Introduction

Diamond is known for its extraordinary thermal conductivity and mechanical hardness, and the production of large-area crystals has been a long term goal. The conventional synthetic methods employed for the production of artificial diamond usually require extremely high pressure and temperature [1,2], or plasma enhanced chemical vapor deposition (CVD) [3,4]. On the other hand, a renewal of interest can possibly originate from the conversion of few layers of graphite (pure form of carbon most familiar as the lead in pencils) into diamond structures. Indeed, the advances today in the growth of large-area graphene [5,6] and bilayer graphene through multilayer graphenes [7-9] would provide this possibility: the chemical conversion of a few layers of graphene into sp^3 bonded diamond-like carbon films. More specifically, the outer surface chemisorption, i.e., hydrogenation or fluorination, of graphene layers deposited on metal surfaces may yield a thermodynamically stable sp^3 -bonded diamond carbon films, as we suggested in this article. We argue that the main driving mechanism can be attributed to the strong hybridization between sp^3 dangling orbital bonds and metallic surface d_z^2 orbitals. These results suggest a method of preparing an ultrathin ‘diamond’ layer over even very large area by conversion of appropriate multilayer graphene on metal surfaces. The obtained diamond films could also be viewed as a carbon based metal-insulator junction that may reveal novel two-dimensional phenomena or as a new type of electronic material, as we also identified for *hexagonal* boron nitride (*h*-BN).

Results and Discussion

It is now well-defined that the graphene layers weakly interact each other by a weak van der Waals (vdW) force forming the graphitic structure with AB stacking layers [10]. The thinnest three-dimensional form of two graphene layers that are deposited on metal surfaces is considered in our study, where the plasma exposure is chemisorbed onto only the outer wall of top layer of bilayer graphene, as shown in Figs. 1(a)–(d). Figure 1(e) shows the thermodynamic stability of the single-side hydrogen and fluorine chemisorption states in bilayer graphene on Ni(111) with respect to the atomic plasma desorbed graphenes, i.e. Stage-I. In the fully functionalized graphene (one of each two carbon is accessible to a functional atom), there are two adsorption sites: Meta [Stages-II (b) and -IV (d)] and Ortho configurations [Stage-III (c)]. As seen in Fig. 1(e), both the hydrogen and fluorine functions show quite similar behavior: The thermodynamics of the functionalized bilayer graphene (Stages-II to -III) are energetically favorable upon the single-side atomic exposure. This could be pursued to our previous studies where the single-side hydrogenation was stabilized in multilayer graphene but that on metallic Co(0001) substrate [11]. In case of double layer graphene, we can exclude the possibility of double-sided functional atoms onto a single layer because the diffusion of functional atoms between the graphene layers is energetically unfavorable. The calculated relative energy indicates that the ortho configuration is the most stable and favored over the meta by about 22 kcal/mol (in

the case of hydrogen), which agrees with the recently reported first principles calculations, in which the hydrogen dimer chemisorbed onto the single-layer graphene was investigated [12]. Furthermore, we also found the local minimum in energy at the meta configuration when the distance between graphene layers is 1.67 Å (Stage-IV). This strong C-C chemical bonding normal to the graphene plane can be the consequence of the structural buckling from the functionalized graphene layer, which conflicts to the typical formation of graphitic layers interacted weakly by physical vdW interaction at larger separation of 3.74 Å. This indicates that there is no significant influence from the metal substrate to the functionalized outer wall of graphene layers, although the metallic surface intends to bind to its adjacent graphene layer with the known strong carbon-p and metal-d hybridization. In contrast, interestingly, the Stage-IV of single-side functionalized bilayer graphene shows a quite fascinating behavior: The Stage-IV has much lower energy (27 kcal/mol) than its physisorption phase of the Stage-II, but also more stable than the ortho configuration (Stage-III) with the energy difference of about 6 kcal/mol. The fluorine binding onto the outer wall of graphenes on metal (C_2F) is slightly more stable than the hydrogen configuration C_2H , as the analogous of the fluorinated graphene compounds.

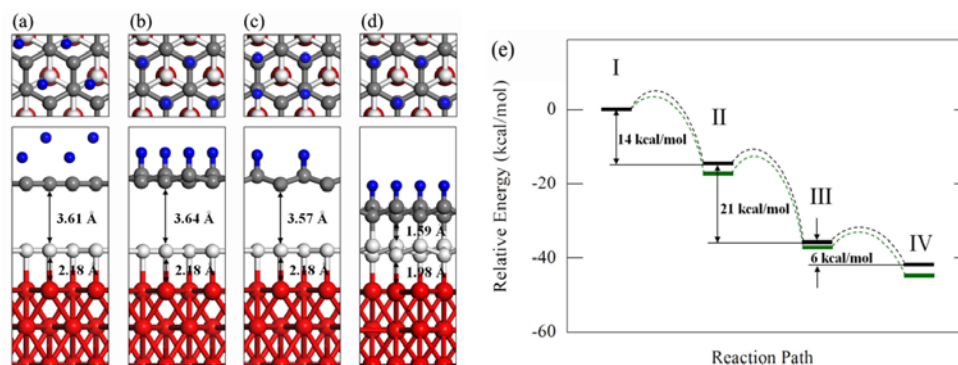


FIG. 1. A sketch of the energetic diagram for the conversion mechanism of sp^2 bilayer graphene on Ni(111) metal surface into sp^3 diamond-like formation upon single-side chemical modifications. (a)–(d) Top and side views of the optimized geometries for Stage-I to –IV: Functional-free graphene Stage-I; Meta-configuration Stage-II; Ortho-configuration Stage-III; sp^3 -bonded meta-configuration Stage-IV. The functionalized graphene layer is depicted in gray, while functional-free graphene layer that is on metal surface (red) is distinguished by white color. Small blue balls are the hydrogen atoms. (e) Relative local minima in potential energy of the hydrogenated (black) and fluorinated (green) bilayer graphenes with respect to the functional-free graphene.

When the chemical functions and metallic substrate are introduced to the both sides of graphite, the sp^2 -bonded C atoms of graphenes can achieve a higher degree of all- sp^3 -bonded diamond: three of the four covalent sp^3 bonds are saturated by carbon atoms and the fourth covalent bond is done by a functional (metal) atom in the upper (lower) graphene layer. In this configuration (Stage-IV), one of every two atomic sublattice of carbon atoms on the upper graphene layer is chemisorbed to functional atoms, and the rest of carbon atoms have covalent bonding with the lower graphene that adsorbed on metal surface with the C-C bond length of 1.58 Å. The $sp^2 \rightarrow sp^3$ conversion further results significant changes in the planar bond lengths and angles between the carbon atoms of the ideal graphite, as shown in Table I. The obtained planar C-C bond length of 1.52 Å is found to be significantly increased from 1.42 Å of graphene, which is similar to the sp^3 bond length (1.53 Å) for diamond. The C-C-C bond angles planar and normal to the graphene plane are 108.5° and 110.2°, which are slightly less and more than a typical bond angle of 109.5° for diamond structure, but much smaller than the known angle of 120° in graphene. The calculated bond lengths for the cases of F exposure are same as those for H-functionalized system, but the angles are slightly modified ($\theta = 109^\circ$ and $\varphi = 109.9^\circ$), which correspond to almost pure sp^3 formation. These results indicate that the present sp^3 formation in our study capture quantitatively the diamond framework, rather than metal-free graphane. Similar phenomenon was achieved for the hydrogenated (or fluorinated) *h*-BN layers on Ni(111) surface, of which the detailed results will be appeared somewhere. We expect that the sp^3 -bonded BN layers exhibit even superior mechanical and electronic properties than the carbon diamond structures.

To understand physical insights underlying the stable $sp^2 \rightarrow sp^3$ conversion upon the metallic surface, we plotted the projected electronic band structure and density of states (DOS) for d-orbitals of Ni and p-orbitals of C atom at the interface in Fig. 2. Figures 2(a) and 2(d) show the majority and minority DOSs for carbon atom at the hydrogenated outer graphene layer, respectively. In contrast to a single graphene layer that displays a semimetallic character with the conical point at K having linear dispersion, the DOS exhibits an insulating nature with the large band gap having similar feature found in diamond structure. To further

examine the graphene-metal interaction, we also analyze the band structures along graphene high-symmetry directions in the Brillouin zone for C and Ni atoms at the interface [Figs. 2(b) and 2(c)]. Further down the distance between the two layers, the system develops strong single covalent bonds, and the bilayer becomes a wide gap semiconductor. Furthermore, the characteristic of Dirac conical points of graphene at K are not identified, while the finite p_z states in the majority spin band at the Fermi level are seen in Fig. 2(b). When graphene is chemisorbed on Ni surface, the graphene bands are strongly perturbed and acquire a mixed p_z - d_z^2 orbitals throughout the energy level. This indicates the strong hybridization between the graphene C and metallic Ni atoms, analogs to the functional-free graphene adsorbed on Ni surface.

TABLE I. Structural properties of bilayer graphene on nickel surface upon the single-side functionalization of hydrogen and fluorine atoms. The corresponding results for pristine bilayer graphene and diamond structures are presented as references of ideal sp^2 and sp^3 bonding, respectively. Here d_1 and d_2 are the C–C bond lengths at lateral and normal to the graphene plane, respectively. φ is the angle formed by the carbon atoms at lateral plane; θ is the angle between the planar and normal bonds to the graphene plane.

Systems	$d(\text{H-C})$	$d_1(\text{C-C})$	$d_2(\text{C-C})$	φ	θ
Graphite	–	1.42	3.74	120	90
H-Bigraphene/Ni	1.11	1.52	1.59	110.2	108.5
F-Bigraphene/Ni	1.38	1.52	1.59	109.9	109.0
Diamond	–	1.53	1.53	109.5	109.5

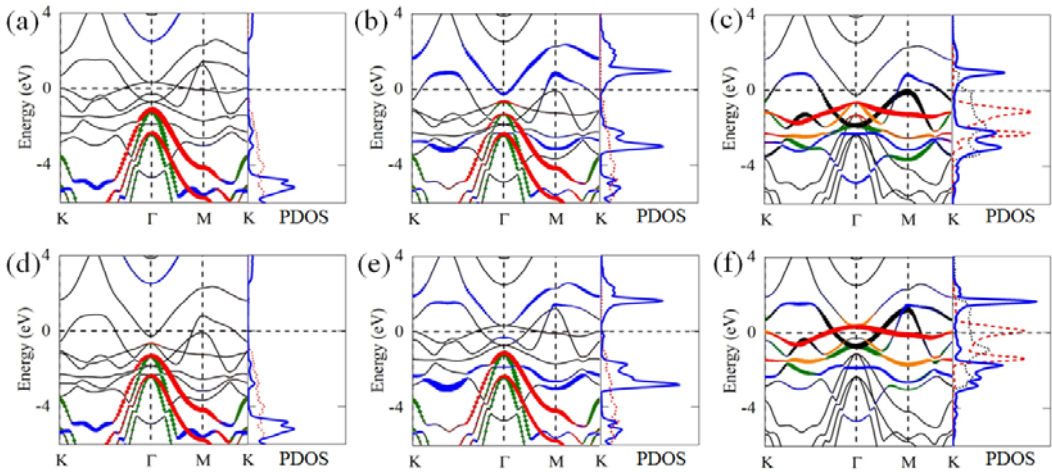


FIG. 2. Electronic band structures and DOS in the majority spin state for C atoms attached to (a) H and (b) Ni, and (c) Ni atom at the interface of the functionalized bilayer graphene on Ni(111) surface. The corresponding states for the minority spin are shown in (d)-(f), respectively. Nickel five d-orbitals of d_{xy} , d_{xz} , d_{yz} , d_z^2 and $d_x^2 - y^2$ states are shown in black, red, orange, blue, and green colors in band structure plots, respectively. The degenerated $d_{xy}/d_x^2 - y^2$, d_{xz}/d_{yz} , and d_z^2 states in DOS are in dotted-black, dashed-red, and solid-blue, respectively. For C-2p states, the red, green, and blue band lines represent the p_x , p_y , and p_z orbitals, respectively, and the dotted black p_x/p_y and solid blue p_z . Fermi level is set to zero energy.

To summarize, the conversion of multilayer graphenes into sp^3 -bonded carbon films on metal surfaces (through hydrogenation or fluorination of the outer surface of the top graphene layer) is indicated. The main driving force for this conversion is the hybridization between sp^3 orbitals and metal surface d_z^2 orbitals. The induced electronic gap states and spin moments in the carbon layers are confined in a region within 0.5 nm of the metal surface. Our results suggest that scaled preparations of multilayer graphene on metal substrates can lead to a fabrication route of very large area ultrathin sp^3 -bonded carbon films that would represent an entirely new carbon material.

References

1. Bundy, F. P., Hall, H. T., Strong, H. M. & Wentorf Jun, R. H. Man-made diamonds. *Nature* 176, 51–55 (1955).
2. Irifune, T., Kurio, A., Sakamoto, S., Inoue, T. & Sumiya, H. Materials: Ultrahard polycrystalline diamond from graphite. *Nature* 421, 599–600 (2003).
3. Bachmann, P. K., Leers, D. & Lydtin, H. Towards a general concept of diamond chemical vapour deposition. *Diamond Relat. Mater.* 1, 1–12 (1991).
4. Isberg, J. et al. High carrier mobility in single-crystal plasma-deposited diamond. *Science* 297, 1670–1672 (2002).
5. Li, X. et al. Large-area synthesis of high-quality and uniform graphene films on copper foils. *Science* 324, 1312–1314 (2009).
6. Bae, S. et al. Roll-to-roll production of 30-inch graphene films for transparent electrodes. *Nature Nanotech.* 5, 574–578 (2010).
7. Wu, Y. et al. Growth mechanism and controlled synthesis of AB-stacked bilayer graphene on Cu–Ni alloy foils. *ACS Nano* 6, 7731–7738 (2012).

8. Li, Q. et al. Growth of adlayer graphene on Cu studied by carbon isotope labeling. *Nano Lett.* 13, 486–490 (2013).
9. Chen, S. et al. Synthesis and characterization of large-area graphene and graphite films on commercial Cu–Ni alloy foils. *Nano Lett.* 11, 3519–3525 (2011).
10. Kim, K. S. et al. Large-scale pattern growth of graphene films for stretchable transparent electrodes. *Nature* 457, 706–710 (2009).
11. Odkhuu, D., Shin, D., Ruoff, R.S. & Park, N. Conversion of multilayer graphene into continuous ultrathin sp³-bonded carbon films on metal surfaces. *Sci. Rep.* 3, 3276–3283 (2013).
12. Han, S. S., et al. Stability of hydrogenation states of graphene and conditions for hydrogen spillover. *Phys. Rev. B* 85, 155408–155414 (2012).

УДК 631.41

doi:10.18.101/978-5-9793-0883-8-116-121

The Using Natural Organic Matter for the Removal Heavy Metals from Contaminated Soil by Electro Kinetic Processes

**Ts. Ochirkhuu¹, Sh. Munkhjargal², B. Khuukhenkhuu¹,
Ts. Bymbasuren¹, G. Ochirbat¹, B. Enkhzul¹**

¹Laboratory of Atomic Spectroscopy, Institute of Physics and Technology, MAS, Mongolia

²Department of Physics, Natural Science Division, School of Arts and Sciences, NUM,

e-mail: Ochko_0525@yahoo.com

Abstract

This work presents the results of removal Pb, Cd, Cu, Zn from mixed soil with natural organic absorbent as gumat and cow manure by electrokinetic processes. By electrokinetic experiment it has been observed that the total contents of Pb, Cd, Cu, Zn in the experimental soils samples were increased depending on electrodes and organic matter mix. The molecular absorption spectrums of hydroxyl, carbonil, carboxyl and phenolic groups arising, shifting and disappear in contaminated soil, soil: gumat, soil: manure mixed samples by treated EK processes.

Keywords: organic matter in soil, soil electro kinetic remedation, heavy metals in soil, cow manure

1. Introduction

Soil is dynamic living system of mixture of minerals, organic matter, gases, liquids, and micro organisms. Soil contamination leads to changing the structure of these components, the interactions and dynamic patterns lost. As for lead, then half of the total amount of the toxicant transferred to the environment from the combustion of leaded petrol car in the city and a motorcycle on pasture field of livestock in rural areas. Heavy metals, into the soil or contained in it, exposed various transformations. The main processes in soil with heavy metals are sorption, migration, transformation, plant uptake, removal of ground water and inclusion in the biogeochemical cycles. Soils have a natural ability to translate part of the heavy metals in the slow-moving state is mainly due to the humus content. As a result of the accumulation intensity of humic substances zinc, copper, lead and cadmium in contaminated soil often exceeds their content background. According to the intensity of accumulation of heavy metals in humus are located in the following order of Cu > Cd > Pb = Co > Ni > Zn > Mn and macroelements (N, P, S, Mg, Fe, K) does not accumulate. Determined that effect of humic substances on the Cu, Pb, Cr (III) leads to the chelating and reduce the toxicity of these heavy metals. Humic substances are formed by the decomposition of plant and animal residues under the action of micro-organisms and abiotic environmental factors are macro-components of organic matter of soil and aquatic ecosystems, as well as solid fuels. Have determined by synchrotron X-Ray analytical techniques that lead a strong connection with a stable gumat and fulvic acid forms more than other heavy metals (*G. M. Varshal 1999*). Most of the literature indicates that with the increase in pH increases the bond strength of heavy metals with organic and mineral components of soil (*B. Gorbatov, 1983, B. Gorbatov, Zyrin NG, 1988, Obukhov, AI et al., 1990*). In particular, xenobiotic as mercury, cadmium, and lead are toxic when not connected to a structures of biomolecules. They are connected to a strong end of the biogroup protein. Humic acid and heavy metals in soil are formed in a stable polymer. Lead metals have slow oxidation and are created carbonate and clay minerals, Fe, Mn and Al oxide to join and connect organic matter. If lead concentration is high, it precipitated in forms of hydroxide, phosphate, carbonate. Soil organic matter has spectral peaks due to alkyl –CH₂ at 2930–2850 cm⁻¹, bands for protein amide OC-NH around 1680 and 1530 cm⁻¹, carboxylate anion –COO- at 1600 and 1400 cm⁻¹, and carboxylic acid COOH around 1720 cm⁻¹ (*Janik et al., 1998*). This makes it easier to formation a lead organic group in complex compounds (*Kabata-Pyendias, Pyendias, 1989, V. Chirita 1994*) and (*E. Chrenekova 1982*) have studied the connection of metals ions to gumus acids of carboxy (SOON), phenol (OH), alcohol (OH), ketones (C = O), amino group (-NH₂), and amido (= NH). At this time, various saturation organic mineral compounds are formed. Have studied the connection to acid and metal ions gumus, carboxy (SOON), phenol